Journal of Solid State Chemistry 182 (2009) 3249–3253

Contents lists available at ScienceDirect

Journal of Solid State Chemistry

journal homepage: www.elsevier.com/locate/jssc

Molten salt synthesis and localized surface plasmon resonance study of vanadium dioxide nanopowders

Fu Wang [a,b], Yun Liu [a], Chun-yan Liu [a,*]

[a] Key Laboratory of Photochemical Conversion and Optoelectronic Materials of Technical Institute of Physics and Chemistry, Chinese Academy of Sciences, Zhongguancun, Beijing 100190, PR China

[b] Graduate School of the Chinese Academy of Sciences, Beijing 100806, PR China

ARTICLE INFO

Article history:
Received 9 June 2009
Received in revised form
7 September 2009
Accepted 12 September 2009
Available online 19 September 2009

Keywords:
Vanadium dioxide
SPR
Nanopowders
KCl–LiCl

ABSTRACT

Rutile-type vanadium dioxide nanopowders with four different sizes were successfully synthesized by carbothermal reducing V_2O_5 in KCl–LiCl molten salt. XRD and TEM characterizations suggested that vanadium dioxide particles formed by a broken and reunited process of vanadium oxide. Molten salt and organic carbon sources are crucial to the size of final particles. In the presence of the molten salt, the organic carbon with a shorter chain length would induce smaller particles. The UV–VIS–IR spectral measurements for as-prepared vanadium dioxide announced an obvious localized surface plasmon resonance band in the near infrared region at 90 °C.

1. Introduction

Vanadium dioxide (VO_2) has six polymorphic forms [1]: tetragonal rutile-type VO_2(R), monoclinic rutile-type VO_2(M), triclinic VO_2(T), and three metastable phases VO_2(A), VO_2(B), VO_2(C). Among them, only VO_2(M) and VO_2(R) undergo a complete reversible semiconductor-metal phase transition at 340 K [2–4], which is accompanied by a drastic change in electrical conductivity and optical transmission [5]. This property enables it promising to be applied in diverse fields such as sensing devices, optical switching devices, optical data storage medium and energy efficiency windows [6–10], et al.

Although many approaches have been explored to fabricate rutile-type VO_2 polycrystalline films, such as sol–gel [11], radio frequency sputtering [12], physical vapor deposition [13], pulsed laser deposition [14], and ion implantation [15]. It is well known that these VO_2 polycrystalline films can not meet the need for coating substrates with large surface area or complex morphology. In comparison with VO_2 polycrystalline thin films, VO_2 nanopowders can not only overcome the disadvantages of films but also have more potential in applications [16], such as plasmonic response in the vicinity of the near-infrared communications wavelengths [17], ferroelasticity and negative mechanical stiffness [18]. To our knowledge, there are several methods have been reported so far on the preparation of rutile-type VO_2 powders, for example, thermal processing [19], hydrothermal reaction [20], pyrolysis of complex precursor [21], evaporative decomposition of solutions technique [22] and laser-induced vapor-phase reaction [23]. However, these techniques are not technically practical in real applications due to the complex control procedure, necessity of the long time reaction or expensive apparatus. Moreover, high temperature treatment required in the most of above fabrication processes would lead to either particles agglomeration or over-growth. Therefore, searching for a simple and reliable synthetic technique is still intriguing and challenging.

In the present work, we have reported a facile method of synthesizing well-dispersed and size-tunable rutile-type VO_2 nanopowders by carbothermal reducing V_2O_5 in KCl–LiCl molten salt. As well known, the molten salt synthesis route has shown excellent performance in synthesizing various inorganic materials, however, it is the first time to be used for the preparation of VO_2. Furthermore, the localized surface plasman resonance (LSPR) character of as-prepared rutile-type VO_2 nanoparticles coated on the surface of SiO_2 was studied as well. Although LSPR of single crystal VO_2(R) [24] and VO_2(R) nanoparticles [25] embedded in an amorphous SiO_2 host have already been known, the variation in coating system is more interesting and promising for practical use.

2. Experimental section

2.1. Reagents and characterization

V_2O_5, Polyvinylpyrrolidone(PVP) K30, sucrose, glucose, KCl and LiCl were all analytical grades and purchased from Beijing Chemical Factory. Deionized water was used in all experiments.

* Corresponding author. Fax: +86 010 62554670.
E-mail address: cyliu@mail.ipc.ac.cn (C.-y. Liu).

0022-4596/$ - see front matter © 2009 Elsevier Inc. All rights reserved.
doi:10.1016/j.jssc.2009.09.014

The carbothermal reaction was carried out in a tube furnace under the protection of N_2. Scanning electron micrograph (SEM) images were obtained on a Hitachi S-4300 scanning electron microscopy. TEM images were obtained on a JEOL JEM-CX200 electron microscope. XRD patterns of the sample were recorded on a Bruker D8 Focus X-ray diffractometer using Cu$K\alpha$ radiation source (λ=1.54056 Å). Optical absorption measurements were carried out by using a Cary 5000 UV–VIS–IR Spectrophotometer, the temperature was controlled by a home-made recycling water-heating setup. Raman spectra were acquired by using Renishaw inVia-Reflex system, excited by 1 W of the 514.5 nm line of an argon ion laser.

2.2. The synthesis of VO_2(M)

We selected three different kinds of organic carbon sources in the carbonthermal reduction (Table 1) and the molar ratio of V to C was 1:0.27, if there was no special illustration. In a typical procedure, 1 g of V_2O_5 and stoichiometrically corresponding carbon source were added into 10 ml deionized water. First, the mixture was stirred for an hour and heated at 80 °C until the water was completely evaporated. Then 14.8 g KCl and 9.7 g LiCl (mol ratio=41:59) were mixed together with the residues, transferred into a planetary ball milling machine and milled for 3 h at the frequency of 25 Hz. The mixture was then placed in an alumina boat in a quartz tube inside a tube furnace. The furnace temperature was increased to 400 °C in 1 h and the sample was annealed at this temperature for 3 h, and then cooled to ambient temperature naturally. The whole process was protected under N_2 (99.999%). The final product was washed with deionized water for several times to remove the salt and then dried in air. In order to make a comparison, VO_2 was also prepared in the absence of the molten salt, kept all the other conditions the same.

Table 1
Experimental conditions and the average size (D) of the sample.

Sample	Carbon source	Molten salt	D_{TEM} (nm)
V_2O_5 (after milling)			400
A	PVP-K30	without	450
B	PVP-K30	KCl–LiCl	130
C	Sucrose	KCl–LiCl	70
D	Glucose	KCl–LiCl	50

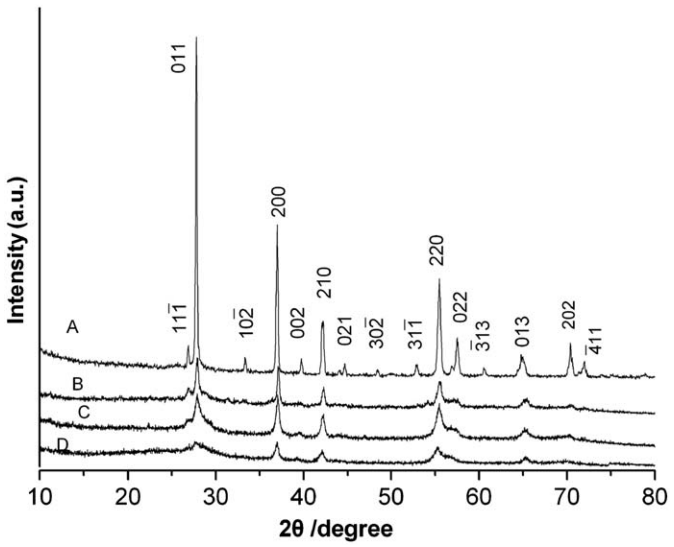

Fig. 1. XRD patterns of the samples: A, B, C, D.

3. Results and discussion

Since most of organic carbon sources were carbonized below 400 °C, the main reaction during the synthesis of the rutile-type VO_2 could be formulated in Eqs. (1) and (2).

$$V_2O_5 + C \rightarrow 2VO_2 + CO \quad (1)$$

$$V_2O_5 + CO \rightarrow 2VO_2 + CO_2 \quad (2)$$

Fig. 1 shows the XRD patterns of sample A, B, C and D. All the reflexes correspond to monoclinic VO_2 (space group $P21/C$) with the lattice constants and the monoclinic angle are a=5.7529 Å, b=4.5263 Å, and c=5.3825 Å, β_M=122.646° (JCPDS file no. 44-0252). No impurity peaks were detected and this proves that all the reactions were completed.

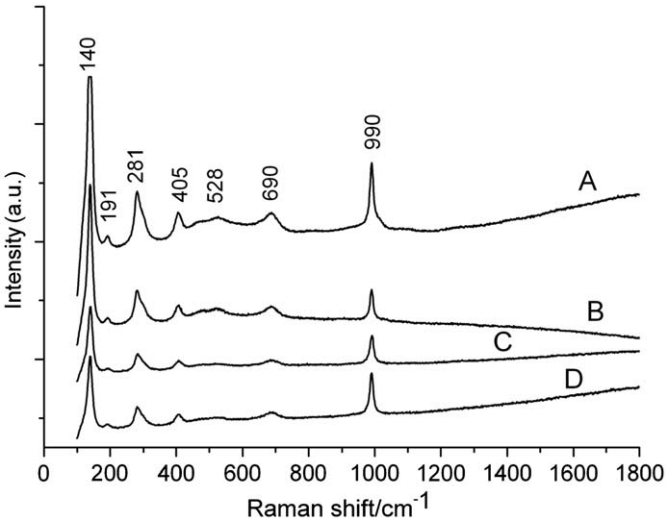

Fig. 2. Raman spectra of the samples: A, B, C, D.

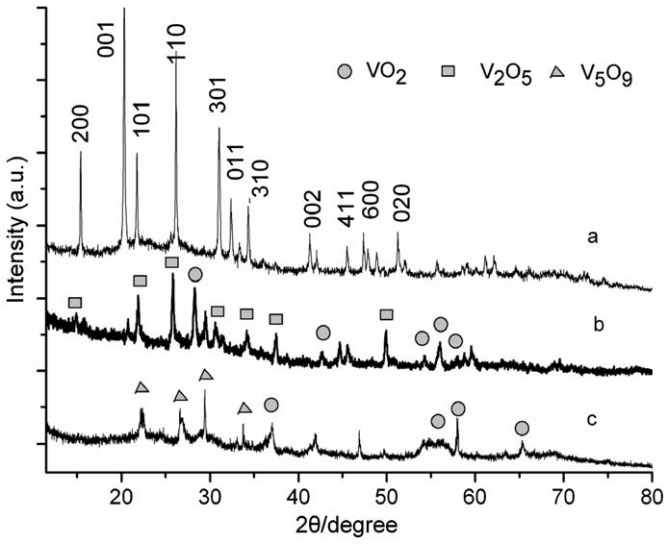

Fig. 3. XRD patterns of V_2O_5 after milling (a), and the product obtained at 370 °C (b) and 450 °C (c) using sucrose as a carbon source.

Fig. 2 presents the Raman spectra of these samples. All the peaks marked in the spectrum are consistent with the previously reported monoclinic VO_2 [26,27]. It is worth noticing that there is no indication of carbon at 1355 cm^{-1} or 1578 cm^{-1}. As the Raman spectroscopy is very sensitive to carbon, we speculate that the products are free of unreacted carbon, which supports the result from XRD.

To explain the influence of temperature and the dose of carbon source during the carbonthermal reduction, we take an example of sucrose as organic carbon source. The dose of sucrose is a little higher than the stoichiometric proportion in order to ensure that all the V_2O_5 can be reduce to VO_2. As shown in Fig. 3b, just a mixture of V_2O_5, VO_2(M) and some unidentified materials were obtained at 370 °C, and the mixture was difficult to transform to pure VO_2(M) by increasing the annealing time. When the temperature was increased up to 450 °C (Fig. 3c), some reflexes corresponding to V_5O_9 appeared (JCPDS file no. 18-1450). This might be ascribed to the enhanced reductibility of some remaining reducing materials at this temperature. When the molar ratio of V to C was further increased to 1:0.6, unreacted carbon begin to emerge in the final products (Fig. 4). As shown in Fig. 4, a typical broad diffraction peak of carbon occurred at about 2θ=25°, while other reflexes were perfectly indexed to monoclinic VO_2. The remaining carbon could not be removed even when increasing the reaction time up to 6 h. However, if the temperature is continuous increased up to 450 °C, the VO_2 is further reduced to V_2O_3 (JCPDS file no. 34-0187), as indicated in Fig. 4.

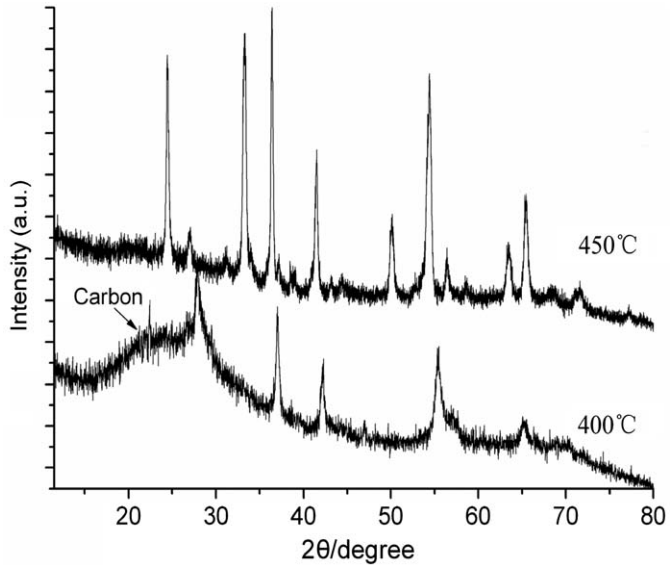

Fig. 4. XRD patterns of the sample prepared at 400 and 450 °C with sucrose as a carbon source.

The milling process did not make V_2O_5 particles smaller (see the supporting information), but could make it well mixed with the molten salt and then prevented the agglomeration of particles during the annealing process. The particles morphology and size distribution of A, B, C and D four samples were characterized by TEM. As displayed in Fig. 5, the products prepared without the molten salt agglomerated into bulk-like-structure of about 450 nm in size. However, the products prepared with molten salt were much smaller and mainly consisted of the separated particles. Interestingly, the size of particles could be controlled in the presence of the molten salt by selecting organic carbon molecules with a different molecular chain length (Table 1).

In order to elucidate the reaction mechanism from bulk V_2O_5 into small VO_2 particles and the effects of the molten salt and organic carbon, a particle growth model in Fig. 6 is proposed. During the preparation process, PVP-K30, sucrose or glucose could serve as capping agents [28–30], and covered on the surface of V_2O_5 particles during the stirring process. As previously reported [28], organic molecules with a longer molecular chain are more effectively adsorbed on the surface of particles than those with the shorter molecular chain. Therefore, the density of the capping layer formed by the longer chain molecules is relatively high. With increasing temperature, the enwrapped carbon coating

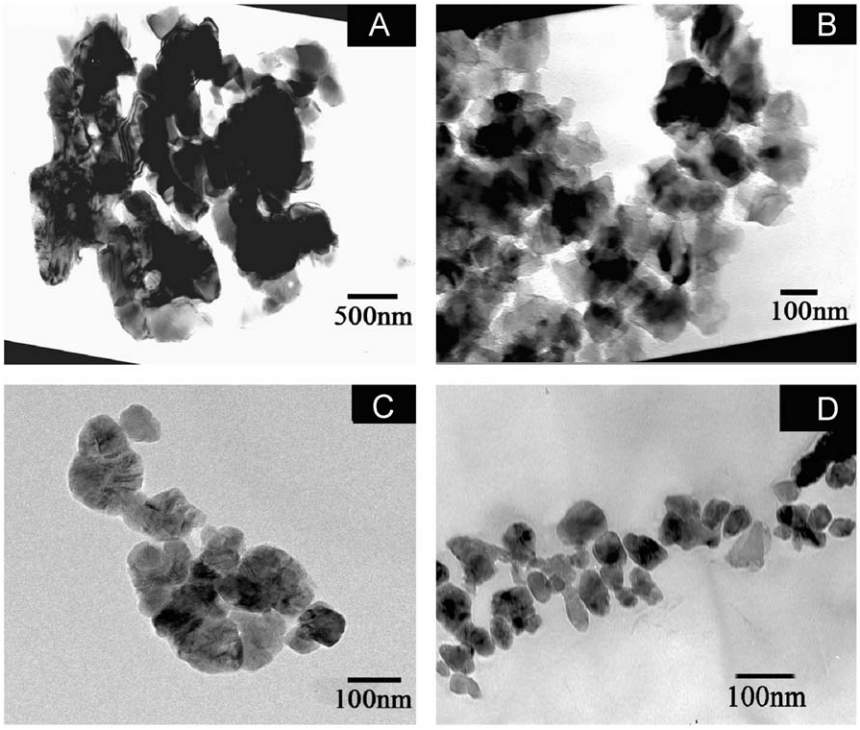

Fig. 5. TEM images of the samples A, B, C, D.

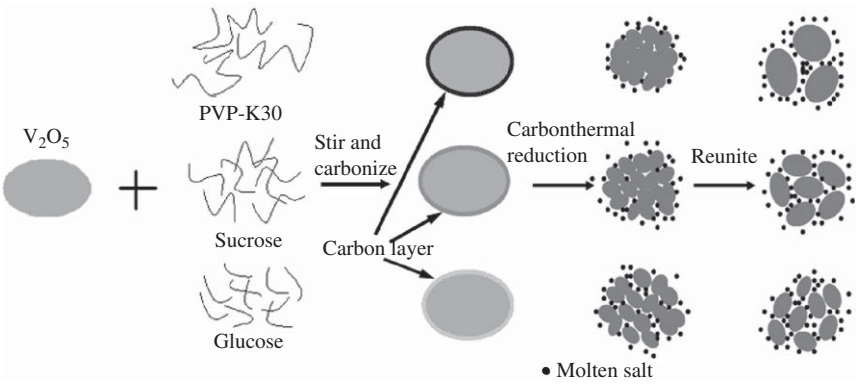

Fig. 6. Schematic illustration of the formation of VO_2(M) nanoparticles.

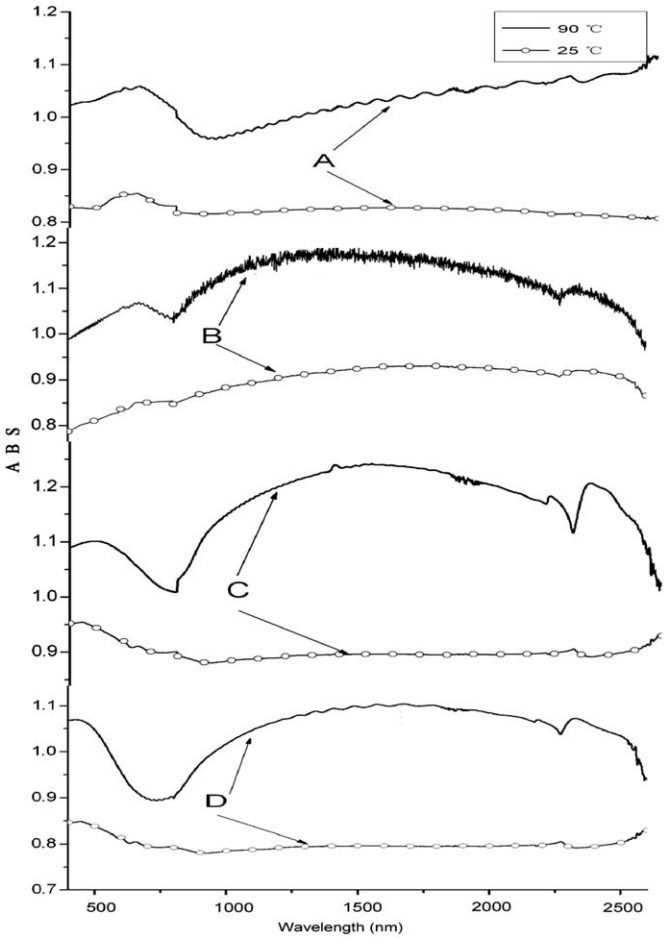

Fig. 7. VIS–NIR absorption spectra of the samples: A, B, C, D under 25 and 90 °C.

would be carbonized, thus denser capping layer formed by longer molecular chain would induce more compact carbon layer. During the reduction reaction, V_2O_5 loses oxygen atoms, so it would rearrange the structure and then break up into smaller VO_2 crystals. However, the compacted carbon layer would hinder the molten salt accessing into the interstice among those crystals, thus resulting in larger VO_2 particles, as the case of PVP-K30 in Fig. 6.

In order to investigate the LSPR of VO_2(R), 20 mg of as-synthesized products were dispersed in 2 ml distilled water. Then the resulted mixtures were coated on a plate of quartz glass ($2 \times 2\,cm^2$) and dried at room temperature. The VIS–NIR absorption spectra of four samples were measured at 25 and 90 °C (Fig. 7). It is obvious that all samples have no absorption at 25 °C, because VO_2 is a semiconductor at that temperature. However, when the temperature increased to 90 °C, semiconductor VO_2 was transformed into a metallic phase. The samples B, C, D showed an obvious broad absorption band in the NIR, but the sample A had no significant absorption band. This might be due to the average size of the sample A is about 450 nm, which is comparable to the interacting light wavelength. Thus it would lead to an inhomogeneous polarization of the nanoparticle by the electromagnetic field [31]. The broadening of LSPR band is then caused by the excitation of different multipole modes with different energies [32]. Moreover, the sample A has a large size distribution and irregular morphology, which can broaden the LSPR position as well.

The insulator-metal transition can be further confirmed by the transmission change in FTIR spectra (see the supporting information). It should be pointed out that the quartz substrates have no absorption in the NIR region in the temperature range. In the present study, the LSPR band had no regular change with size decreasing. This is probably due to the fact that the LSPR is not only sensitive to the particles sizes but also the composition, morphology, and surrounding dielectric media of the particles. As reported in previous research [33], the LSPR of hemisphere-like Ag occurred at 506 nm, however, the LSPR of Ag triangle was at 654 nm.

4. Conclusions

The present study demonstrates a facile and scalable method to prepare rutile-type VO_2 and it might be a general approach for the synthesis of other similar types of materials. The reaction temperature and the amount of reducing agents are crucial to the formation of rutile-type VO_2. All factors of ball milling, organic carbon source, molten salts play an important role in the control of the product size. A model was also proposed to illustrate the carbothermal reaction. Attempts to obtain the LSPR of VO_2(R) dispersed in a solvent were hindered due to the fact that most of solvents have a stronger absorption after 1400 nm; fortunately, a broad absorption band in NIR region from the sample loaded on a quartz glass was observed. The LSPR band showed here broadened, this was probably due to non-optimum condition of as-prepared samples. Therefore further study is needed to synthesize monodispersed and uniform rutile-type VO_2 particles to make their LSPR large enough to be suitable in practical applications.

Acknowledgments

The author thanks to the support of National Natural Foundation of China (20773151), 973 Program and Chinese Academy of Sciences.

Appendix A. Supplementary material

Supplementary data associated with this article can be found in the online version at doi:10.1016/j.jssc.2009.09.014.

References

[1] Z. Gui, R. Fan, X.H. Chen, Y.C. Wu, J .Solid State Chem. 157 (2001) 250–254.
[2] F.J. Morin, Phys. Rev. Lett. 3 (1959) 34–36.
[3] C.N.R. Rao, C.N. Rao, B. Raveau, Transition Metal Oxides, Wiley-Interscience, New York, 1995.
[4] J.B. Goodenough, J. Solid State Chem. 3 (1971) 490–500.
[5] K.D. Rogers, J.A. Coath, M.C. Lovell, J. Appl. Phys. 70 (1991) 1412–1415.
[6] H.T. Kim, B.G. Chae, D.H. Youn, G. Kim, K.Y. Kang, Appl. Phys. Lett. 86 (2005) 242101–242103.
[7] S.H. Chen, H. Ma, X.J. Yi, H.C. Wang, X. Tao, M.X. Chen, X.W. Li, C.J. Ke, Infrared Phys. Technol. 45 (2004) 239–242.
[8] J.C.C. Fan, H.R. Fetterman, F.J. Bachner, P.M. Zavracky, C.D. Parker, Appl. Phys. Lett. 31 (1977) 11–13.
[9] W.E. Case, J.L. Smith, D.D. Eden, Proc. SPIE—Int. Soc. Opt. Eng. 168 (1983) 420–425.
[10] M.A. Sobhan, R.T. Kivaisi, B. Stjerna, C.G. Granqvist, Sol. Energy Mater. Sol. Cell 44 (1996) 451–455.
[11] I. Takahashi, M. Hibino, T. Kudo, Jpn. J. Appl. Phys. 40 (2001) L1367–L1369.
[12] W. Burkhardt, T. Christmann, B.K. Meyer, W. Niessner, D. Schalch, A. Scharmann, Thin Solid Films 345 (1999) 229–235.
[13] C. Piccirillo, R. Binions, I.P. Parkin, Thin Solid Films 516 (2008) 1992–1997.
[14] G. Garry, O. Durand, A. Lordereau, Thin Solid Films 453 (2004) 427–430.
[15] P. Jin, S. Nakao, S. Tanemura, Thin Solid Films 324 (1998) 151–158.
[16] J. Nag, R.F. Haglund Jr., J. Phys. Condens. Matter 20 (2008) 264016–264030.
[17] M. Rini, A. Cavalleri, R.W. Schoenlein, R. L'opez, L.C. Feldman, J.R.F. Haglund, L.A. Boatner, T.E. Haynes, Opt. Lett. 30 (2005) 558–560.
[18] R.S. Lakes, T. Lee, A. Bersie, Y.C. Wang, Nature 410 (2001) 565–567.
[19] K.F. Zhang, X. Liu, Z. Xing, L.H. Li, Mater. Lett. 61 (2007) 2644–2647.
[20] C.X. Cao, Y.F. Gao, H.J. Luo, J. Phys. Chem. C 112 (2008) 18810.
[21] C.M. Zheng, J.L. Zhang, G.B. Luo, J.Q. Ye, M.M. Wu, J. Mater. Sci. 35 (2000) 3425–3429.
[22] S.A. Lawton, E.A. Thby, J. Am. Ceram. Soc. 78 (1995) 104–108.
[23] O. Toshiyuki, I. Yasuhiro, R.K. Kenkyu, J. Photopolym. Sci. Technol. 10 (1997) 211–216.
[24] A. Bianconi, S. Stizza, R. Bernardini, Phys. Rev. B 24 (1981) 4406–4411.
[25] R. Lopez, T.E. Haynes, L.A. Boatner, Opt. Lett. 27 (2002) 1327–1329.
[26] B.W. Mwakikunga, S.E. Haddad, M. Maaza, Opt. Mater. 29 (2007) 481–487.
[27] X.C. Wu, Y.R. Tao, L. Dong, Z.H. Wang, Z. Hu, Mater. Res. Bull. 40 (2005) 315–321.
[28] S. Jeong, K. Woo, D. Kim, S. Lim, J.S. Kim, H. Shin, Y.N. Xia, J. Moon, Adv. Funct. Mater. 18 (2008) 679–686.
[29] J.C. Liu, P. Raveendran, G.W. Qin, Y. Ikushima, Chem. Commun. (2005) 2972–2974.
[30] J.C. Liu, M. Anand, C.B. Roberts, Langmuir 22 (2006) 3964–3971.
[31] L. Stephan, A.E. Mostafa, J. Phys. Chem. B 103 (1999) 8410–8426.
[32] C.F. Bohren, D.R. Huffman, Absorption and Scattering of Light by Small Particles, Wiley, New York, 1983.
[33] X. Zhang, E.M. Hicks, J. Zhao, G.C. Schatz, R.P. Van Duyne, Nano Lett. 5 (2005) 1503–1507.